Article

Machine Learning Models for Inferring the Axial Strength in Short Concrete-Filled Steel Tube Columns Infilled with Various Strength Concrete

Ngoc-Tri Ngo[1,a,*], Hoang An Le[2,b], Van-Vu Huynh[1,c], and Thi-Phuong-Trang Pham[3,d]

1 The University of Danang – University of Science and Technology, Danang, Vietnam
2 NTT Hi-Tech Institute, Nguyen Tat Thanh University, Hochiminh, Vietnam
3 The University of Danang – University of Technology and Education, Danang, Vietnam

E-mail: [a,*]trinn@dut.udn.vn (Corresponding author), [b]lhan@ntt.edu.vn, [c]vuhuynh.dtmt@gmail.com, [d]ptptrang@ute.udn.vn

Abstract. Concrete-filled steel tube (CFST) columns are used in the construction industry because of their high strength, ductility, stiffness, and fire resistance. This paper developed machine learning techniques for inferring the axial strength in short CFST columns infilled with various strength concrete. Additive Random Forests (ARF) and Artificial Neural Networks (ANNs) models were developed and tested using large experimental data. These data-driven models enable us to infer the axial strength in CFST columns based on the diameter, the tube thickness, the steel yield stress, concrete strength, column length, and diameter/tube thickness. The analytical results showed that the ARF obtained high accuracy with the 6.39% in mean absolute percentage error (MAPE) and 211.31 kN in mean absolute error (MAE). The ARF outperformed significantly the ANNs with an improvement rate at 84.1% in MAPE and 65.4% in MAE. In comparison with the design codes such as EC4 and AISC, the ARF improved the predictive accuracy with 36.9% in MAPE and 22.3% in MAE. The comparison results confirmed that the ARF was the most effective machine learning model among the investigated approaches. As a contribution, this study proposed a machine learning model for accurately inferring the axial strength in short CFST columns.

Keywords: Machine learning, random forests, concrete-filled steel tube columns, data analytics.

1. Introduction

Bridges, buildings, and support structures have used concrete-filled steel tube (CFST) columns because of the superiority of CFST columns such as high strength, ductility, stiffness, and fire resistance [1]. Various studies have concerned the behavior of CFST columns. For example, the performance of CFST columns reinforced externally and internally by spirals was evaluated [2]. They used sixteen CFST samples to test under axial compression and the samples were stiffened externally continuous spirals (ECS), internal continuous spiral (ICS), and unwelded internal continuous spiral (UICS). This research showed that toughness and elastic strength were enhanced remarkably when stiffening the CFST columns were stiffened externally and internally by spirals. ECS, ICS, and UICS enhanced the compressive capacity of 46.8 percent, 48.7 percent, and 47.9 percent, respectively, as compared to the benchmarking sample.

Another study we can mention is researching the behavior of CFST short columns and beam with initially imperfect concrete [3]. This work studied the impact of the gap on the mechanical behavior of compression and bending of CFST structures and the authors tested data of twenty-one experimental specimens, consists of fourteen short columns subjected to axial compressive loading and seven beams subjected to bending. Furthermore, Zhu et al presented the behavior in CFST structures subjected to influence of axial load and axial influence tests of twelve CFST columns were experimented [4].

Steel-fiber-reinforced recycled aggregate concrete (RAC) in manufacturing CFST columns was researched in this study [5]. Their study evaluated the axial behavior of fifty-four steel-fiber-reinforced self-stressing the RAC-filled steel tube (SSRCFST) column. The study also proposed formulations to predict the ultimate capacity of SSRCFST columns and compared them with experimental results. The performance of concrete-filled stainless steel tube (CFSST) stub columns was researched in [6]. They investigated nine concrete-filled austenitic stainless-steel tubes (austenitic CFSST) and nine concrete-filled duplex stainless-steel tubes (duplex CFSST) stub columns. Finally, new methods were proposed to improve the prediction of strength for the austenitic and duplex CFSST structures.

An empirical method was proposed for estimating the stability of special-shaped CFST columns under the axial force [7]. The ABAQUS tool has been applied to build finite element models. The estimated results from the proposed method were aligned with the recorded data and they were relatively smaller than the results of the finite element method [7]. A model was established for multi-cell CFST (MCFST) columns under axial load [8]. The proposed model calculated the load-deformation curves of 12 samples with various shapes as well as structures and compute the constitutive relationship of concrete in every cell individually. The findings revealed that the model provides useful guidance for the MCSFT column.

Recycled aggregate concrete can be considered a useful way to handle waste disposal as well as yield benefits for environmentally sustainable development. A prediction model was created for inferring the compressive strength in RAC-filled steel tube columns [9]. The proposed model is also compared to the ANNs model and the previous empirical methods to demonstrate the good performance of the model.

Concrete strength (CS) can be considered as an important factor that is essential for designing concrete structures. Therefore, there is a diversity of research studied the CS. Particularly, a new optimized self-learning model was created for inferring CS in high-performance concrete [10]. Besides, circular ultra-high performance concrete-filled steel tube columns (UHPC-FSTCs) was reviewed and analyzed to provide a useful reference to the compressive behavior of UHPC-FSTCs under axial load [11]. Talaat et al reviewed the factors that affect the results of concrete compression to demonstrate the complex of it [12]. The authors showed that there are three major factors affecting compressive strength of concrete. They were the size of specimens, shape, and friction. These major factors impact the recorded phenomena, and they influence each other. Xu et al applied machine learning-based model for predicting CS of Ready-Mix concrete [13].

Moreover, the behavior of confinement of ultra-high-performance concrete without and with the use of steel fibers (UHPC and UHPFRC) was researched [14]. In this research, the authors studied circular steel tube confined concrete (STCC) columns infilled with the UHPC and UHPFRC with concrete strength between one hundred fifty MPa and two hundred MPa. Several studies about STCC columns with UHPC and UHPFRC have been conducted [15-17]. Therefore, it is necessary to study CFST columns with different strength concrete including high strength and ultra high strength concrete with or without steel fibers.

Recently, machine learning techniques have been applied to solving engineering problems in civil engineering [18, 19]. For instance, the artificial neural networks (ANNs) model is one of the main powerful tools in machine learning and is commonly used for a wide variety of problems. The study proposed a model based on the ANNs algorithm and it was able to predict the strength of FRP-confined concrete [20]. The proposed model also was compared with international codes and analytical models and the results showed that the model was suitable for the design of FRP-confined concrete and enhanced the accuracy of the available competitors.

ANNs models were applied in forecasting the capacity of circular short CFST columns under short-term axial load with a large number of experimental data [21]. They showed that the proposed formular was able to precisely forecast the ultimate strength of columns with axial load. Besides, the ANNs was combined with case-based reasoning (CBR) system to forecast the dynamic properties of ultra-high-performance concrete (UHPC) [22]. The results evidence showed that the proposed intelligent system could predict various mechanical properties of UHPC with varied combinations and yielded overall prediction accuracy of the system was 81.5% [22].

The random forests (RF) is effective and accurate for solving regression problems with high complexity because it produces a dozen of decision trees and integrates them to generate outputs [23]. For example, it was applied to predict internal damage in reinforced concrete [24] and predict building energy use profiles [25]. The additive RF (ARF) is an enhanced version of RF that can improve its performance [26]. Few studies investigate the machine learning models for CFST columns infilled with various strength concrete. Besides, because of the superiority of ANNs and ARF models, this study examines their effectiveness and applicability in inferring the axial strength in short CFST columns infilled with normal strength concrete (NSC), high strength (HSC), high strength (HSC), and ultra-high-strength concrete (UHSC).

As a contribution, this study proposed a machine learning model to infer the axial strength in short CFST columns. Machine learning models were trained and tested to propose an effective machine learning model for inferring the axial strength in short CFST columns. Due to the limited test data, this study extended the behavior of CFST columns with a variety of strength concrete types. A large dataset of experimental tests for circular CFST short columns was collected. Moreover, the performance of investigated machine learning model was compared with those of empirical design codes such as Euro code 4 [27] and American code AISC 2010 [28] to demonstrate that the proposed model outperformed another model and experimental results.

2. Research Methodology

2.1. Additive Random Forests

RF models were developed by Breiman [29] that are effective machine learning models [30]. Therefore, there are variety of researchers applying RF in their studies. For example, Han et al used RF Algorithm in machine fault diagnosis. This paper aims to present a method that rotates machinery faults can be diagnosed. And the method is based on the RF model, a novel assemble model that can build a huge amount of decision trees to enhance on the individual tree model [31]. Moreover, other researchers used RF to evaluate fault detection in bioreactor operation [32]. The authors give the position that it is very vital to determine the faults in a live process to avoid product quality deterioration and they have focused on the process history-based methods to identify the faults in bioreactors. In this study, they introduced the RF model, a powerful machine learning model, to detect fault types in a bioreactor. In biological field, RF was used to analyze surface-enhanced Raman scattering data [33]. The RF integrated various decision trees to reduce the variance of the RF without exposing the residual. RF involves bagging and a random feature subset. Figure 1 shows the architecture of RF for inferring the axial strength of CFST columns. The training phase of a randomly created forest is started data resample by a bootstrap method, then growing a tree for each data point

and divide among a random specific subset of inputs, that is the tuning parameter of RF models. This rule was repeated until C trees were grown.

Giving the RF model is a group of C trees $T_1(X)$, $T_2(X),\ldots,$ $T_C(X)$, in which $X = x_1,$ $x_2,\ldots,x_m$ is the m-dimension input vector. The group generates C outcomes as Eq. (1)

$$Y_{pred\_1} = T_1(X), Y_{pred\_2} = T_2(X), \ldots, Y_{pred\_C} = T_C(X) \quad (1)$$

where Y_{pred_C} is the predicted values.

The result of those created trees was combined to get finally an output Y_{pred_C} that was the average values of whole trees in forests. The RF produced C number of decision trees from N training data points. Bootstrap sampling was deployed to produce the training set and test set [34, 35]. The training data was applied to build an unpruned regression tree. This process was repeated until C decision trees were grown to form a randomly created forest.

The ARF is an improved version of RF that was used in this study. The ARF model is a metamodel that improves the accuracy of a regression base model. Each generation fits a model to the difference left by the RF on the previous generation. Regression was done with the addition of the results of each model. This improves a smoothing effect [26].

2.2 Artificial Neural Networks

An ANNs model is a common machine learning model that has been applied for engineering problems such as prediction of groundwater level in hard rock region [36] and pavement engineering [37]. Cong et al presented a comprehensive review of the applications of ANNs in flow and heat transfer problems in nuclear engineering [38]. Particularly, this study, the authors applied ANNs for inferring the flow regime, pressure drop, void fraction, critical heat flux, onset of nucleate boiling, heat transfer coefficient and boiling curve has been reviewed, respectively.

Figure 2 presents the three-layer architecture of the ANNs model. The multilayers in the ANNs were trained by the back-propagation method that can improve the power in solving complex problems [39]. The back-propagation method can effectively optimize connected weights and error values in learning ANNs models. Activated neurons of hidden-output layers are as Eq. (2).

$$net_k = \sum w_{kj} o_j \quad \text{and} \quad y_k = f(net_k) \quad (2)$$

where net_k is the activated function of the kth neuron; j is the neuron in the previous layer; w_{kj} is the connected weight of neurons k and j; o_j is the output, and y_k is the sigmoid or logistic transferring function.

$$f(net_k) = \frac{1}{1 + e^{-\lambda net_k}} \quad (3)$$

where λ controls the function gradient.

The w_{kj} was trained and updated using Eq. (4) as below

$$w_{kj}(t) = w_{kj}(t-1) + \Delta w_{kj}(t) \qquad (4)$$

The change value $\Delta w_{kj}(t)$ is

$$\Delta w_{kj}(t) = \eta \delta_{pj} o_{pj} + \alpha \Delta w_{kj}(t-1) \qquad (5)$$

where η is the learned value; δ_{pj} are propagating errors; o_{pj} is the output of neuron j for record p; a is the momentum value, and $\Delta w_{kj}(t\text{-}1)$ are the changing values in in the preceding iteration.
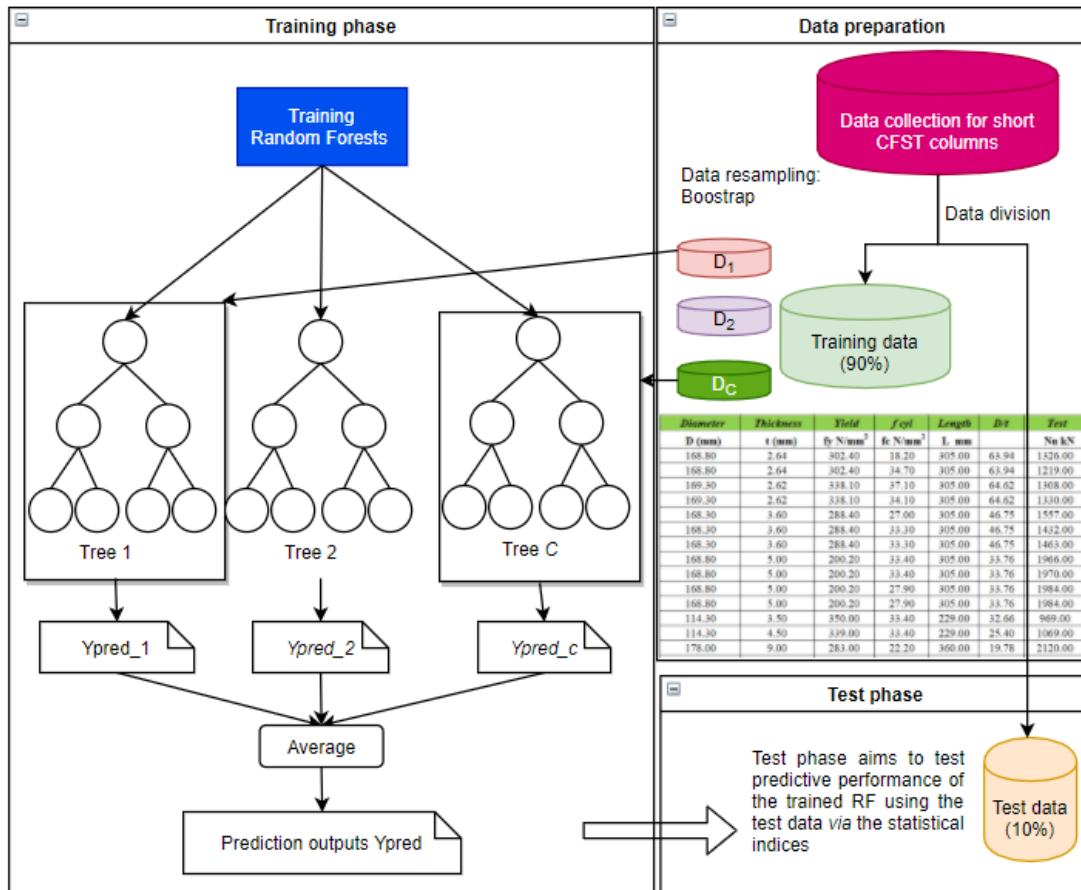

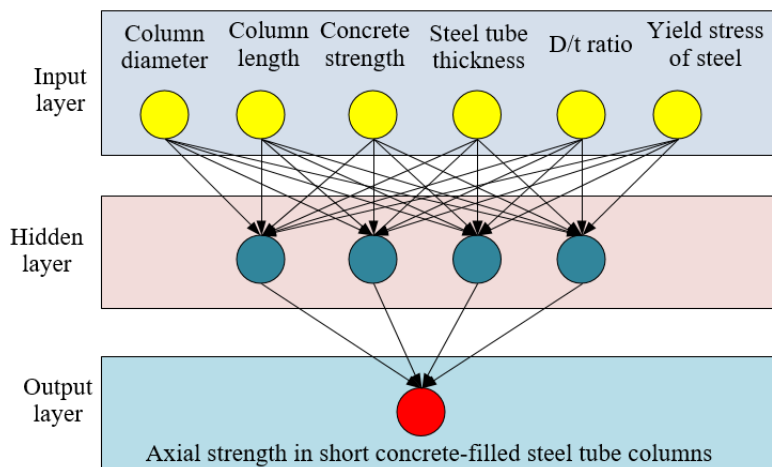Fig. 1. Random Forests: Training and test processes.

Fig. 2. Architecture of ANNs for inferring the axial strength in short CFST columns.

3. Analytical Results

3.1. Data Preparation

Data in this study were retrieved from the ASCCS [40]. Data of 802 CFST columns infilled with NSC, HSC, and UHSC were used to develop the machine learning models and evaluate their performance. Data attributes were presented in Table 1 that includes the diameter (D), steel tube thickness (t), steel yield stress (f_y), compressive strength of concrete (f_c), length (L), D/t, and the axial strength in CFST columns (N_u).

Table 1. Summary of data attributes.

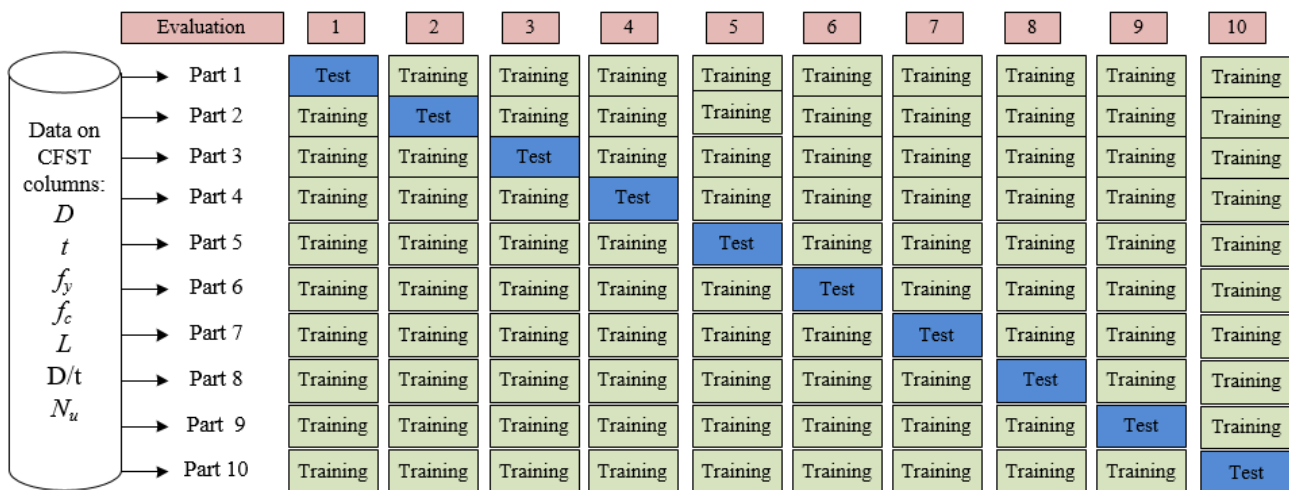| Statistics	D (mm)	t (mm)	f_y (N/mm2)	f_c (N/mm2)	L (mm)	D/t	N_u (kN)
Average	174.5	4.4	359.4	62.9	506.1	48.6	3095.7
Standard deviation	109.7	2.5	111.2	37.1	314.0	34.2	4476.6
Minimum	48.0	0.5	181.4	9.9	150.0	9.0	106.0
Maximum	1020.0	16.5	853.0	193.3	3060.0	220.9	46000.0

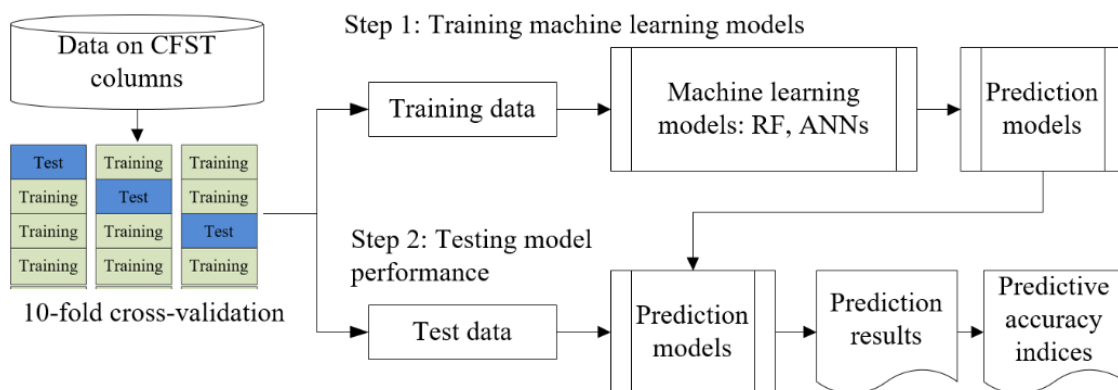Fig. 3. Data resampling by the k-fold cross-validation method.

Fig. 4. Training and testing process for machine learning models.

3.2. Model Training and Testing Results

The 802-sample data were divided randomly into ten folds using the k-fold cross-validation method as shown in Fig. 3. Figure 4 illustrates the training and testing process of the ANNs model and ARF model. The machine learning techniques were trained and tested ten times by the training and test data. The training data were constituted by nine parts while the test data were constituted by one remaining part. Particularly, the set of

the training data to train the models and the test set to test the models. The testing step helps to find out the best model being suitable with selected data. After the machine learning models were trained, the test data were fed into the trained models to produce the predicted values of the axial strength in CFST columns. Those prediction results were compared against the actual values of the axial strength in CFST columns via statistical indices to evaluate model performance.

Predictive accuracy of the machine learning model was measured *via* statistical indices that consist of MAE, MAPE, and R. Formulation of these indices was presented as Eqs. (6) – (8)

$$MAE = \frac{1}{n} \sum_{i=1}^{n} |y - y'| \qquad (6)$$

$$MAPE = \frac{1}{n} \sum_{i=1}^{n} \left| \frac{y - y'}{y} \right| \qquad (7)$$

$$R = \frac{n \sum y.y' - (\sum y)(\sum y')}{\sqrt{n(\sum y^2) - (\sum y)^2} \sqrt{n(\sum y'^2) - (\sum y')^2}} \qquad (8)$$

where y' are inferred data; y are measured data; and *n* is database size.

Table 2 presents the parameter settings of machine learning models as default values. For the ANNs model, the hidden layer is set as 4, the learning rate is 0.3, and the momentum is 0.2. For the ARF model, the percent of the bag size is 100, the number of features is 0 while predictors or inputs equal 6, and maxDepth is 0 that means the maximum depth of the tree is unlimited. These settings were suggested by Weka, an open-source machine learning software [41]. Figure 5 depicts the relationship between the measured and inferred values of the compressive strength of the short CFST members. The visualization shows that the measured data and inferred outputs by the ANNs and ARF models are quite close to the diagonal line. They are a good agreement between them. Table 3 summarizes the numeric results of ANNs and ARF models. Table 4 shows the predictive results obtained by the ARF and ANNs models in one evaluation. The predictive accuracy obtained by the ANNs was 610.44 kN of the MAE. The predictive accuracy obtained by the ANNs was 610.44 kN of MAE, 40.26 % of MAPE, and 0.980 of R. The ARF yielded the 211.31 kN in MAE, 6.39%

in the MAPE, and 0.980 in R Accuracy comparison results confirmed that the ARF outperformed the ANNs in inferring the axial strength of short CFST infilled with NSC, HSC, and UHSC

Table 2.   Parameter settings of ANNs and ARF models.

Model	Default parameter settings
ANNs	Hidden layer = 4; Training rate = 0.3; Momentum = 0.2 .
ARF	bagSizePercent = 100; numFeatures = 0; maxDepth = 0 (The max depth of the tree, 0 for unlimited.)

The performance of machine learning models was also compared with those of the empirical methods such as EC4 [27] and AISC 2010 [28] in inferring the axial strength of CFST columns. Figure 6 plots the prediction results obtained by EC4 and AISC codes. As shown in Table 3, the EC4 and AISC 2005 achieved a competitive performance in the prediction. The EC4 was more effective than the AISC 2010 in inferring the axial strength in CFST columns. The MAPE values were 10.12 % and 19.71 % by the EC4 and the AISC codes, respectively.

The comparison among machine learning models and design codes in Table 3 showed that the power of the proposed ARF model was better than that of the ANNs model, EC4, and AISC codes for inferring the axial strength of the short CFST column. The enhancement rate by the ARF was 65.4 % in MAE and 84.1 % in MAPE as compared to the ANNs model. Compared to design codes, the ARF model improved 22.3 – 64.0 % in MAE and 36.9 – 67.6 % in MAPE. Figures 7 - 9 present comparisons of the MAE, MAPE and R among these models and design codes. Figure 10 and 11 visualizes the improvement rate obtained by the ARF model as compared to the ANNs model, the AISC codes, and the EC4 code The comparison revealed the effective performance of the ARF model in the inference. Therefore, the findings in this study suggest the application of the ARF model in inferring the axial strength of the short CFST columns. Besides, the study contributes to the application promotion of machine learning and artificial intelligence in the civil engineering domain. For practical applications, the proposed model can facilitate civil engineers or design in quickly and effectively infer the compressive strength of CFST columns.

Table 3.   Predictive accuracy of machine learning models and design codes.

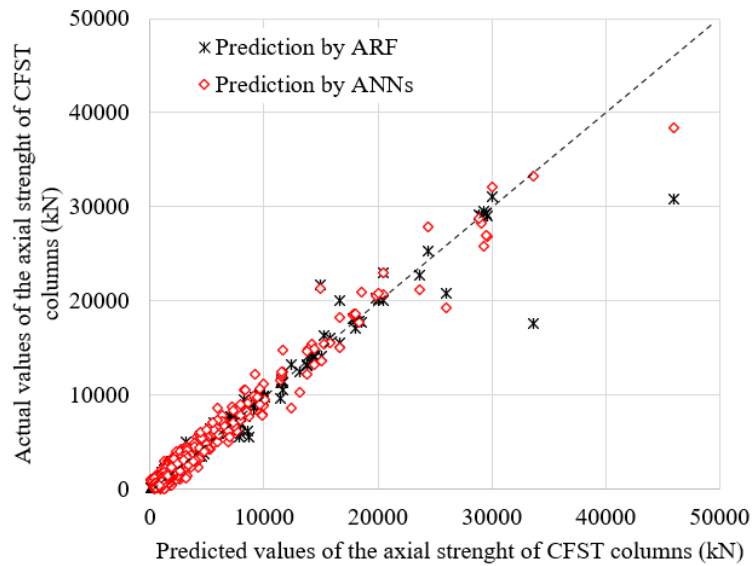| Prediction method	Predictive accuracy			Enhancement rate by the ARF		
	R	MAE (kN)	MAPE (%)	R	MAE	MAPE
ANNs	0.980	610.44	40.26	0.0%	65.4%	84.1%
EC4	0.992	272.08	10.12	-1.2%	22.3%	36.9%
AISC	0.990	587.49	19.71	-1.0%	64.0%	67.6%
Proposed ARF	**0.980**	**211.31**	**6.39**			

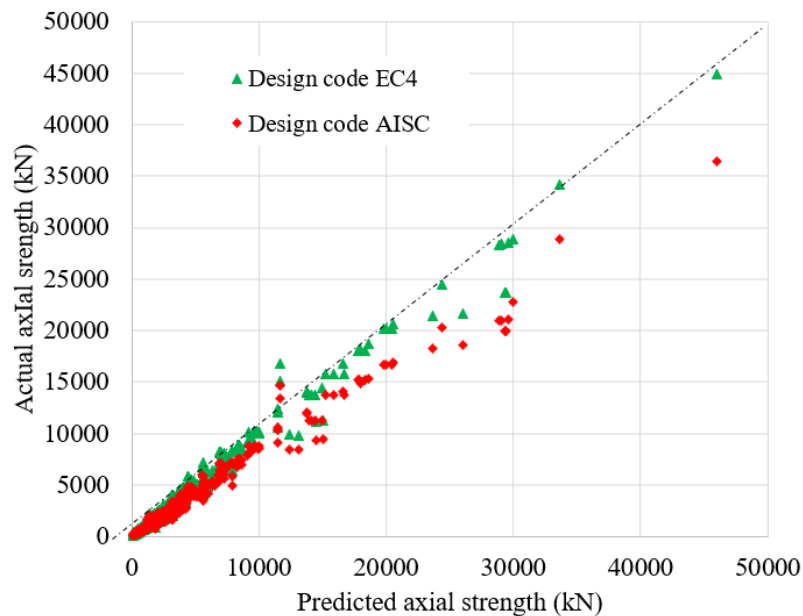Fig. 5. Prediction results by machine learning models.

Fig. 6. Prediction results by design codes.

Table 4. Predictive results of machine learning models in one evaluation.

| No.	Actual N_u (kN)	Predicted N_u (kN) by ARF model	Predicted N_u (kN) by ANNs model	No.	Actual N_u (kN)	Predicted N_u (kN) by ARF model	Predicted N_u (kN) by ANNs model
1	1537	1551.8	2311.5	42	1818.6	1877.7	2050.3
2	2075	2061.3	2856.1	43	1967	2049.8	2137.7
3	2730	2719.9	3804.3	44	29294	29456.6	25800.8
4	4102	3943.5	5495.6	45	2107	1856.8	2518.3
5	2740	3087.6	4187.9	46	112	108.5	966.5
6	5578	5572.8	6219.2	47	7222	6400.7	8743.6
7	8594	6189.0	9156.7	48	1367	2111.9	2256.1
8	1962	1993.2	3053.1	49	1073.1	1086.5	1606.9
9	16670	15543.8	14997.0	50	2080	1829.1	3126.9
10	134	129.7	931.2	51	1068	1089.7	1912.0
11	1496	1499.7	2308.8	52	1359	1767.0	2127.5
12	1500	1471.7	2186.6	53	4350	4213.0	5884.3
13	1813	1879.4	1942.5	54	4547	3468.1	5039.1
14	2040.2	2041.4	3310.5	55	7933	6852.8	9024.1
15	1612	1624.0	2146.5	56	5638	5713.7	6551.5
16	2480	2349.8	3207.3	57	14161	14187.6	15438.1
17	1300	1179.2	1914.0	58	2110	2066.7	3193.5
18	11481	9646.6	11543.2	59	3647	3613.3	4313.0
19	840	875.0	1573.9	60	485	375.1	1288.2
20	3851	3234.3	4559.3	61	1220	1221.7	2105.1
21	1140	1122.7	1867.9	62	715	710.7	1494.5
22	1540	1497.9	2234.7	63	2440	2333.1	3166.4
23	1030	1125.3	1787.8	64	2186	2189.8	1997.7
24	29590	29007.7	26862.2	65	3025	3275.3	4061.9
25	539	467.7	1349.7	66	2037	2036.5	2384.2
26	2070	1829.1	3126.9	67	1042	1090.2	1701.9
27	2070	2070.7	3354.1	68	1191	1193.9	2006.4
28	1699	1581.6	2415.7	69	1200	1174.7	2051.7
29	2957	3098.8	3993.4	70	2077	2069.3	3439.1
30	1509	1284.7	2191.7	71	1821	1783.3	2932.6
31	2100	1973.0	2461.3	72	2055	2078.1	2862.0
32	2832	2736.5	3982.5	73	1323	1348.4	2231.5
33	5390	5068.5	6198.8	74	3420	3239.2	3787.3
34	1408	1428.6	2209.4	75	3193	3155.4	2876.0
35	1647	1583.5	2507.8	76	5241	6360.1	5936.9
36	1925	1908.7	1997.3	77	1849	1823.4	1961.5
37	3152	3278.7	4489.1	78	2177	2177.3	2515.6
38	1620	1621.8	2208.3	79	904	890.0	1736.3
39	1379	1520.9	1930.7	80	2926	2607.8	3903.2
40	465	457.8	1149.0	81	822	845.3	1598.3
41	13092	12413.2	10248.8				
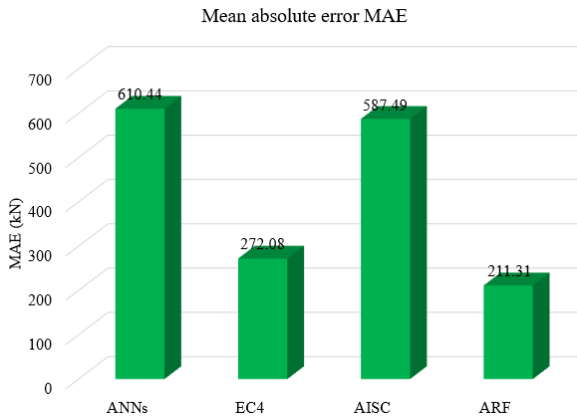
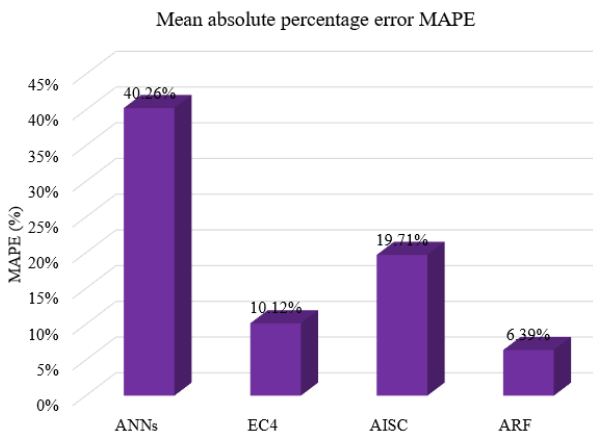Fig. 7. MAE comparison of predictive models and design codes.

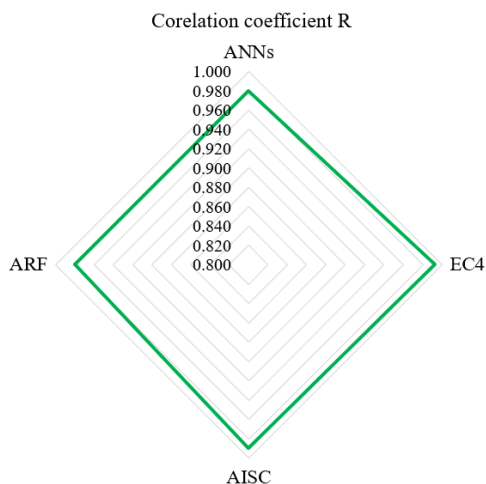Fig. 8. MAPE comparison of predictive models and design codes.

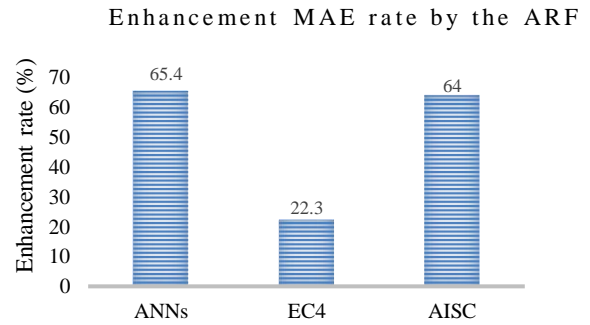Fig. 9. Correlation coefficient comparison of prediction models and design codes.

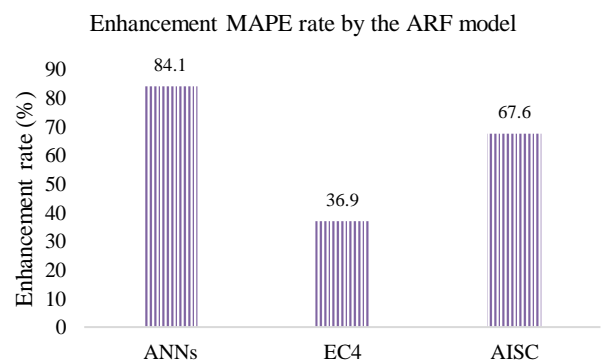Fig. 10. Enhancement MAE rate by the ARF compared to ANNs, EC4 and AISC.

Fig. 11. Enhancement MAPE rate by the ARF compared to ANNs, EC4 and AISC.

4. Conclusions

The study proposed a machine learning technique for inferring the axial strength of short CFST columns. Notably, the ANNs and ARF techniques were investigated in this study. Their performance was compared with the codes of EC4 and AISC 2010. The CFST columns consist of normal strength concrete (NSC), high strength concrete (HSC), or ultra-high-strength concrete (UHSC).

The ANNs and ARF were examined ten times to ensure generalizability in the prediction. The comparison results confirmed the ARF model achieved outstanding accuracy with 211.31 kN in mean absolute error and 6.39% in the mean absolute percentage error. The enhancement rate by the ARF model was 65.4 % in MAE and 84.1 % in MAPE as compared to the ANNs model. Compared to design codes, the ARF model improved 22.3 – 64.0 % in MAE and 36.9 – 67.6% in MAPE.

As a contribution of this study, the ARF was proposed as an effective alternative for inferring the axial strength in short CFST columns that can help civil engineers or designers in designing CFST columns. This study also promoted the application of machine learning models in the civil engineering field. As a limitation of the study, the limited size of CFST columns was used to develop prediction models. Future studies may collect

additional datasets of CFST columns to provide more accuracy in prediction. Besides, future studies should consider optimizing the parameters of prediction models to enhance model performance.

Acknowledgement

References

[1] L.-H. Han, W. Li, and R. Bjorhovde, "Developments and advanced applications of concrete-filled steel tubular (CFST) structures: Members," *Journal of Constructional Steel Research*, vol. 100, pp. 211-228, 2014.

[2] S. K. Alrebeh and T. Ekmekyapar, "Structural behavior of concrete-filled steel tube short columns stiffened by external and internal continuous spirals," *Structures*, vol. 22, pp. 98-108, 2019.

[3] F.-Y. Liao, L.-H. Han, and S.-H. He, "Behavior of CFST short column and beam with initial concrete imperfection: Experiments," *Journal of Constructional Steel Research*, vol. 67, pp. 1922-1935, 2011.

[4] Y. Zhu, H. Yang, X. Yang, and F. Sun, "Behavior of concrete-filled steel tubes subjected to axial impact loading," *Journal of Constructional Steel Research*, vol. 173, p. 106245, 2020.

[5] Z. Liu, Y. Lu, S. Li, and S. Yi, "Behavior of steel tube columns filled with steel-fiber-reinforced self-stressing recycled aggregate concrete under axial compression," *Thin-Walled Structures*, vol. 149, p. 106521, 2019.

[6] P. Dai, L. Yang, J. Wang, and Y. Zhou, "Compressive strength of concrete-filled stainless steel tube stub columns," Engineering Structures, vol. 205, p. 110106, 2020.

[7] X. Chen, T. Zhou, Z. Chen, J. Liu, and B. Jiang, "Mechanical properties of special-shaped concrete-filled steel tube columns under eccentric compression," *Journal of Constructional Steel Research*, vol. 167, p. 105779, 2019.

[8] F. Yin, S.-D. Xue, W.-L. Cao, H.-Y. Dong, and H.-P. Wu, "Behavior of multi-cell concrete-filled steel tube columns under axial load: Experimental study and calculation method analysis," *Journal of Building Engineering*, vol. 28, p. 101099, 2020.

[9] A. I. Nour and E. M. Güneyisi, "Prediction model on compressive strength of recycled aggregate concrete filled steel tube columns," *Composites Part B: Engineering*, vol. 173, p. 106938, 2019.

[10] Y. Yu, W. Li, J. Li, and T. Nguyen, "A novel optimised self-learning method for compressive strength prediction of high performance concrete," *Construction and Building Materials*, vol. 184, pp. 229-247, 2018.

[11] A. L. Hoang and E. Fehling, "A review and analysis of circular UHPC filled steel tube columns under axial loading," *Structural Engineering and Mechanics*, vol. 62, no. 4, pp. 417-430, 2017.

[12] A. Talaat, A. Emad, A. Tarek, M. Masbouba, A. Essam, and M. Kohail, "Factors affecting the results of concrete compression testing: A review," *Ain Shams Engineering Journal*, 2020.

[13] J. Xu, L. Zhou, G. He, X. Ji, Y. Dai, and Y. Dang, "Comprehensive machine learning-based model for predicting compressive strength of ready-mix concrete," Materials, vol. 14, p. 1068, 2021.

[14] A. H. Le, F. Ekkehard, D. K. Thai, and C. V. Nguyen, "Simplified stress-strain model for circular steel tube confined UHPC and UHPFRC columns," *Steel and Composite Structures*," vol. 29, pp. 125-138, 2018.

[15] A. Le Hoang and E. Fehling, "Effect of steel fiber on the behavior of circular steel tube confined UHPC columns under axial loading, in *International Conference on Strain-Hardening Cement-Based Composites*, Springer, Dordrecht, 2017, pp. 482-491.

[16] A. Le Hoang, E. Fehling, D. K. Thai, and C. Van Nguyen, "Evaluation of axial strength in circular STCC columns using UHPC and UHPFRC," *Journal of Constructional Steel Research*, vol. 153, pp. 533-549, 2018.

[17] A. Le Hoang, B. Lai, D.-K. Thai, and N. Chau, "Experimental study on structural performance of UHPC and UHPFRC columns confined with steel tube," *Engineering Structures*, vol. 187, pp. 457-477, 2019.

[18] A.-D. Pham, N.-T. Ngo, and T.-K. Nguyen, "Machine learning for predicting long-term deflections in reinforce concrete flexural structures," *Journal of Computational Design and Engineering*, vol. 7, no. 1, pp. 95-106, 2020.

[19] J.-S. Chou and N.-T. Ngo, "Engineering strength of fiber-reinforced soil estimated by swarm intelligence optimized regression system," *Neural Computing and Applications*, vol. 30, pp. 2129-2144, 2018.

[20] A. Cascardi, F. Micelli, and M. A. Aiello, "An Artificial Neural Networks model for the prediction of the compressive strength of FRP-confined concrete circular columns," *Engineering Structures*, vol. 140, pp. 199-208, 2017.

[21] M. Ahmadi, H. Naderpour, and A. Kheyroddin, "Utilization of artificial neural networks to prediction of the capacity of CCFT short columns subject to short term axial load," *Archives of Civil and Mechanical Engineering*, vol. 14, no. 3, pp. 510-517, 2014.

[22] M. R. Khosravani, S. Nasiri, D. Anders, and K. "Weinberg Prediction of dynamic properties of ultra-high-performance concrete by an artificial intelligence approach," Advances in Engineering Software, vol. 127, pp. 51-58, 2019.

[23] Y. Zhu, W. Xu, G. Luo, H. Wang, J. Yang, and W. Lu, "Random Forest enhancement using improved

Artificial Fish Swarm for the medial knee contact force prediction," *Artificial Intelligence in Medicine*, vol. 103, p. 101811, 2020.

[24] P.-J. Chun, I. Ujike, K. Mishima, M. Kusumoto, and S. Okazaki, "Random forest-based evaluation technique for internal damage in reinforced concrete featuring multiple nondestructive testing results," *Construction and Building Materials*, vol. 253, p. 119238, 2020.

[25] A.-D. Pham, N.-T. Ngo, T. T. Ha Truong, N.-T. Huynh, and N.-S. Truong, "Predicting energy consumption in multiple buildings using machine learning for improving energy efficiency and sustainability," *Journal of Cleaner Production*, vol. 260, p. 121082, 2020.

[26] J. H. Friedman, "Stochastic gradient boosting," *Computational Statistics & Data Analysis*, vol. 38, pp. 367-378, 2002.

[27] *Design of Composite Steel and Concrete Structures, Part 1.1, General Rules and Rules for Building*, BS EN 1994-1-1, British Standards Institution, London, UK, 2004.

[28] *Specification for Structural Steel Buildings*, U.S. 360-10, AIoSCAA, An American National Standard, 2010.

[29] L. Breiman, "Random forests," *Machine Learning*, vol. 45, pp. 5-32, 2001.

[30] X. Qiu, L. Zhang, P. N. Suganthan, and G. A. Amaratunga, "Oblique random forest ensemble via Least Square Estimation for time series forecasting," *Information Sciences*, vol. 420, pp. 249-262, 2017.

[31] X. D. T. Han, B.-S. Yang, and S.-J. Lee, "Application of random forest algorithm in machine fault diagnosis," in *Engineering Asset Management*, J. Mathew, J. Kennedy, L. Ma, A. Tan, and D. Anderson, Eds. London: Springer, 2006, pp. 779-784.

[32] R. Shrivastava, H. Mahalingam, and N. N. Dutta, "Application and evaluation of random forest classifier technique for fault detection in bioreactor operation," *Chemical Engineering Communications*, vol. 204, pp. 591-598, 2017.

[33] S. Seifert, "Application of random forest based approaches to surface-enhanced Raman scattering data," *Scientific Reports*, vol. 10, p. 5436, 2020.

[34] M. W. Ahmad, M. Mourshed, and Y. Rezgui, "Trees vs Neurons: Comparison between random forest and ANN for high-resolution prediction of building energy consumption," *Energy and Buildings*, vol. 147, pp. 77-89, 2017.

[35] R. Jiang, W. Tang, X. Wu, and W. Fu, "A random forest approach to the detection of epistatic interactions in case-control studies," *BMC Bioinformatics*, vol. 10, no. Suppl 1, 2009, art. no. S65.

[36] M. K. Mayilvaganan and K. B. Naidu, "Application of artificial neural network for the prediction of groundwater level in hard rock region," in *International Conference on Computational Science, Engineering and Information Technology*, 2011, pp. 673-682.

[37] M. Abambres and A. Ferreira, *Application of ANN in Pavement Engineering: State-of-Art.* 2017.

[38] T. Cong, G. Su, S. Qiu, and W. Tian, "Applications of ANNs in flow and heat transfer problems in nuclear engineering: A review work," *Progress in Nuclear Energy*, vol. 62, pp. 54-71, 2013.

[39] F. Rosenblatt, *Principles of Neurodynamics: Perceptrons and the Theory of Brain Mechanisms*. Washington, DC: Spartan Books, 1961.

[40] ASCCS AoS-CCS, "ASCCS composite columns database," University of Bradford, Bradford, West Yorkshire, BD7 1DP, UK, 2019.

[41] University of Waikato. *Weka—An Open-Source Machine Learning.* (2020).

Ngoc-Tri Ngo, photograph and biography not available at the time of publication.

Hoang An Le, photograph and biography not available at the time of publication.

Van-Vu Huynh, photograph and biography not available at the time of publication.

Thi-Phuong-Trang Pham, photograph and biography not available at the time of publication.